

## The impedance of thin dense oxide cathodes

Bernard A. Boukamp<sup>a,\*</sup>, Nicolas Hildenbrand<sup>a</sup>, Pieter Nammensma<sup>b</sup>, Dave H.A. Blank<sup>a</sup>

<sup>a</sup> University of Twente Dept. of Science and Technology & MESA<sup>+</sup> Institute for Nanotechnology, P.O.Box 217, 7500AE Enschede, The Netherlands

<sup>b</sup> Energy Centre Netherlands, P.O. Box 1, 1755ZG Petten, The Netherlands

### ARTICLE INFO

#### Article history:

Received 1 September 2009

Accepted 26 May 2010

Available online 29 June 2010

#### Keywords:

Impedance

MIEC

SOFC cathode

PLD

LEISS

### ABSTRACT

The impedance is derived for a dense layer electrode of a mixed conducting oxide, assuming that the electronic resistance may be ignored. The influence of layer thickness, oxygen diffusion and surface exchange rate on the 'General Finite Length Diffusion' expression is evaluated. The thickness dependence is tested for a series of thin, dense layer electrodes of  $\text{La}_{0.6}\text{Sr}_{0.4}\text{Co}_{0.2}\text{Fe}_{0.8}\text{O}_{3-\delta}$  (LSCF) deposited on a  $\text{Ce}_{0.9}\text{Gd}_{0.1}\text{O}_{1.95}$  electrolyte by pulsed laser deposition (PLD). A minimum thickness is required to avoid the influence of contact points of the contacting Pt-gauze and sheet resistance, which is about  $1\ \mu\text{m}$  for the studied LSCF electrodes. LEISS surface analysis indicates that PLD deposition process easily leads to a significant Cr contamination of the LSCF surface. Electrochemical impedance spectroscopy analysis indicates that the influence on the exchange rate of this Cr-contamination is still negligible.

© 2010 Elsevier B.V. All rights reserved.

### 1. Introduction

Mixed conducting oxides (MIEC's) are finding important application in solid oxide fuel cells (SOFC), both as cathode and anode, and in semi-permeable membranes for (partial) oxidation reactions. A very important aspect of these applications is the transfer and reduction of ambient oxygen at the gas/solid interface, or *visa versa*. The overall transfer reaction can be presented as:



But in reality it will involve a series of steps, e.g. adsorption, dissociation, charge transfer and possibly surface diffusion. So far the exact reaction mechanism is still poorly understood. Another significant problem is the exact nature of the surface and the possibility of poisoning by foreign atoms. This is especially of significance for SOFC cathodes where chromium poisoning, which originates from the steel interconnect plates, has been recognized as a serious problem.

Using oxygen isotope ( $^{18}\text{O}_2$ ) exchange the overall exchange rate can be determined. SIMS depth profiling can yield both the tracer diffusion coefficient and the exchange rate [1]. Gas phase analysis in a closed system [2] or in a newly developed pulse technique [3], can yield reaction rates for a two step mechanism, but requires the use of powders. Conductivity relaxation measurements [4,5] can also provide the exchange rate and chemical diffusion coefficient, but sample

dimensions must be carefully chosen [6]. A third option is the study of a thin layer of the MIEC, deposited on an appropriate electrolyte in a three electrode configuration with electrochemical impedance spectroscopy (EIS) [7]. The advantage of such a system is that the study of the influence of surface poisoning can be carried out quite easily. A proper derivation of the impedance of such an electrode arrangement is not readily available in literature. In this contribution a simple model is derived for the impedance of a thin layer and is applied to a dense  $\text{La}_{0.6}\text{Sr}_{0.4}\text{Co}_{0.2}\text{Fe}_{0.8}\text{O}_{3-\delta}$  (LSCF) electrode layer, deposited with pulsed laser deposition (PLD) on a Gd-doped ceria electrolyte. The influence of the layer thickness on the electrode property is studied and some preliminary results on chromium addition are presented.

### 2. Theory

#### 1. Generic finite length diffusion (GFLD) equation

Fig. 1 presents schematically the electrochemical process in a thin dense oxide layer (MIEC) which is on one side connected to an oxygen conducting electrolyte ( $x=0$ ) and on the other side to the ambient (with fixed  $p\text{O}_2$  at  $x=l$ ). The following assumptions are made:

- The electronic conductivity is large enough to be ignored in the derivation.
- The electrode voltage, with respect to a reference electrode at the same ambient  $p\text{O}_2$  is controlled by the oxygen activity in the MIEC at the  $x=0$  interface.
- The oxygen exchange rate can be represented with a single reaction rate,  $k$  (dimension:  $\text{cm}\cdot\text{s}^{-1}$ ).
- Charge transfer and double layer charging processes at the electrolyte/MIEC interface are not included.

\* Corresponding author.

E-mail address: [B.A.Boukamp@UTwente.nl](mailto:B.A.Boukamp@UTwente.nl) (B.A. Boukamp).

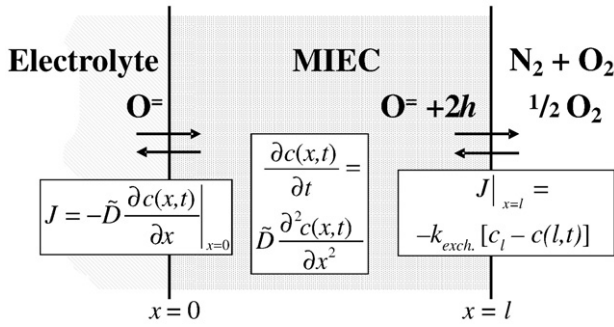


Fig. 1. Reaction schematic for the oxygen transfer through a MIEC layer.

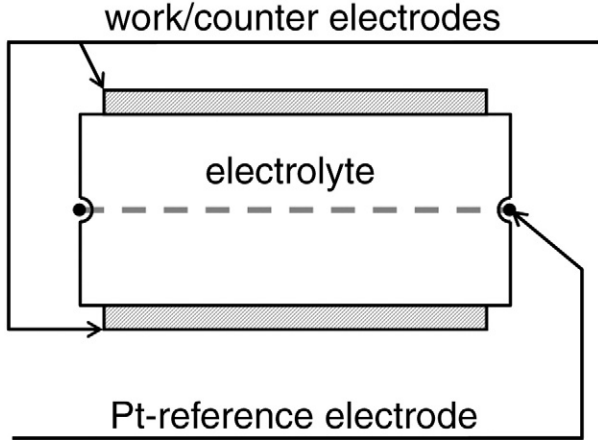


Fig. 2. Schematic arrangement of the three electrode cell with two PLD layers.

The Fickian diffusion equations are:

$$J = -\tilde{D} \frac{\partial c(x,t)}{\partial x} \Big|_{x=0} \text{ and } : \frac{\partial c(x,t)}{\partial t} = \tilde{D} \frac{\partial^2 c(x,t)}{\partial x^2} \quad (2)$$

The right-hand boundary condition at  $x=l$  is given by:

$$J|_{x=l} = -\tilde{D} \frac{\partial c(x,t)}{\partial x} \Big|_{x=l} = -k_{exch.} [c_l - c(l,t)] \quad (3)$$

where  $c_l$  is the (apparent) equilibrium concentration in the ambient. With electrochemical impedance spectroscopy only a small perturbation is applied, hence it is useful to define the concentration variation,  $\Delta c(x,t)$ :

$$\Delta c(x,t) = c(x,t) - c_0^\circ \quad (4)$$

Here  $c_0^\circ$  is the equilibrium oxygen concentration, hence  $c_l = c_0^\circ$ . After transformation of the diffusion equations to the Laplace space, a general solution for Eq. (2) can be given:

$$C(x,p) = A \cosh x \sqrt{p/\tilde{D}} + B \sinh x \sqrt{p/\tilde{D}} \quad (5)$$

with  $p$  the Laplace variable. Inserting (5) in the boundary condition Eq. (3) yields a relation between the coefficients  $A$  and  $B$ :

$$B = -A \frac{\sqrt{p\tilde{D}} + k_{exch.} \coth l \sqrt{p/\tilde{D}}}{\sqrt{p\tilde{D}} \cdot \coth l \sqrt{p/\tilde{D}} + k_{exch.}} \quad (6)$$

The current at  $x=0$  is, after Laplace transformation of Eq. (2), defined by:

$$I(p) = n \cdot F \cdot S \cdot J(p) = -n \cdot F \cdot S \cdot B \sqrt{p\tilde{D}} \quad (7)$$

where  $n$  is the charge of the diffusing ion ( $n=2$  for oxygen),  $F$  is the Faraday constant and  $S$  is the surface area. The electrode voltage is directly related to the oxygen activity,  $a_O(x,p)$ , which is the sum of the equilibrium value and the electrochemical perturbation,  $a_O(x,p) = a_0^\circ + a(x,p)$ . This is expressed in Laplace space with:

$$V(p) = \frac{RT}{nF} \ln \left( \frac{a_0^\circ + a(x,p)}{a_0^\circ} \right) \Big|_{x=0} \approx \frac{RT}{nF a_0^\circ} a(x,p)_{x=0} \quad (8)$$

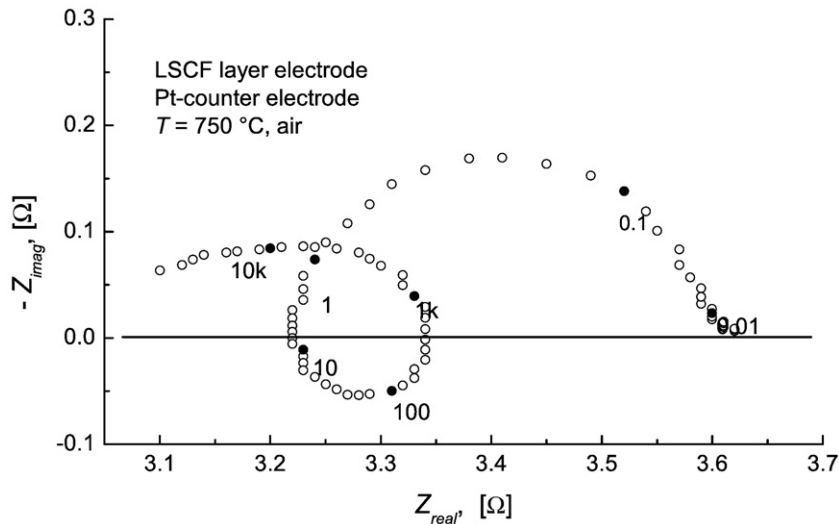


Fig. 3. Inductive artefact in the electrode impedance in a three-electrode cell with a porous Pt electrode with a significant larger polarisation resistance than the LSCF working electrode.

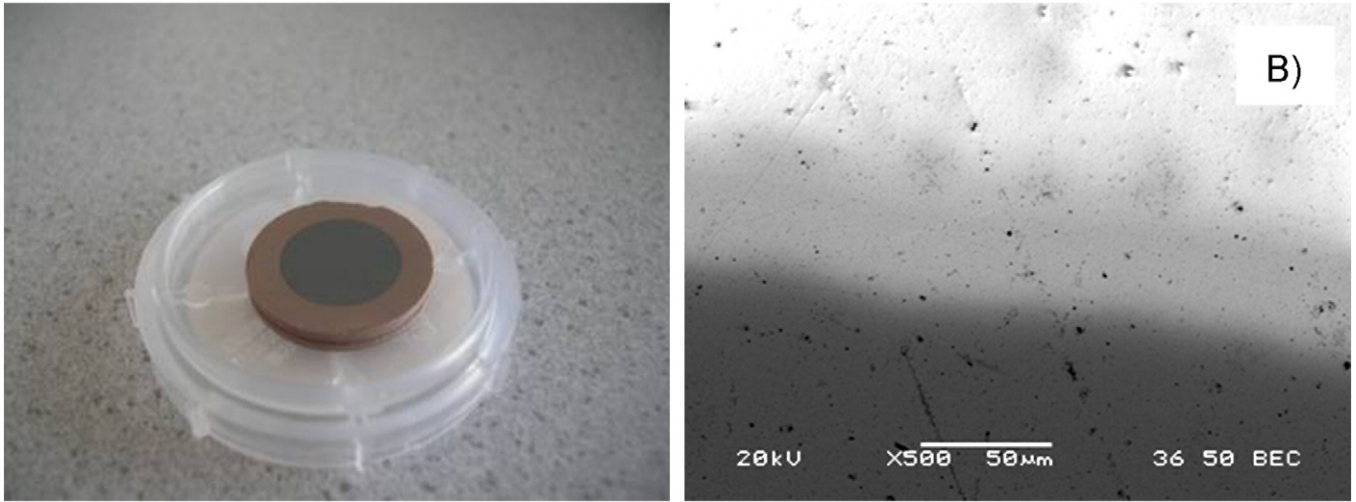


Fig. 4. Photograph of a PLD LSCF layer on a CGO electrolyte (left) and a SEM image of the LSCF surface (right).

assuming that the perturbation is much smaller than the equilibrium activity. The relation between concentration and activity is given by the thermodynamic enhancement factor,  $W$ :

$$W = \frac{\partial \ln c}{\partial \ln a} = \frac{c}{a} \cdot \frac{\partial a}{\partial c} \quad (9)$$

This factor can be obtained from TGA or coulometric titration experiments. Now Eq. (8) can be expressed in  $C(x,p)$  by combining Eqs. (8) and (9):

$$V(p) = \frac{RT}{nF c_i^0} \left[ \frac{\partial \ln a_0^0}{\partial \ln c_0^0} \right] C(x,p)_{x=0} = \frac{RT}{nF c_i^0} \left[ \frac{\partial \ln a_0^0}{\partial \ln c_0^0} \right] A \quad (10)$$

Dividing the voltage by the current yields the impedance in Laplace space. Assuming steady state conditions,  $j\omega$  can be substituted for the Laplace variable  $p$ , resulting in the final impedance equation for the 'GFLD':

$$Z(\omega) = \frac{Z_0 \sqrt{j\omega \tilde{D}} \coth l \sqrt{j\omega / \tilde{D}} + k_{exch.}}{j\omega \tilde{D} k_{exch.} \coth l \sqrt{j\omega / \tilde{D}} + \sqrt{j\omega \tilde{D}}} \quad (11)$$

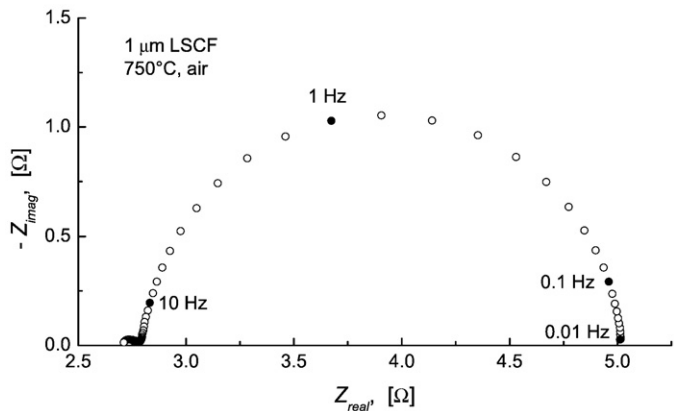


Fig. 5. Typical impedance diagram for a 1 µm thick PLD LSCF layer, 750 °C in air.

With:

$$Z_0 = \frac{RT}{n^2 F^2 S c_0^0} \left[ \frac{\partial \ln a_0^0}{\partial \ln c_0^0} \right] = \frac{RT}{8 F^2 S c_0^0} \left[ \frac{\partial \ln P_{O_2}}{\partial \ln c_0^0} \right] \quad (12)$$

The high frequency limit yields the well-known Warburg or semi-infinite diffusion relation. It is easy to see that for very fast surface exchange ( $k \rightarrow \infty$ ) Eq. (11) simplifies to the finite length Warburg (FLW, [8,9]), while for blocking conditions ( $k=0$ ) the finite space Warburg (FSW, [8,9]) evolves.

The low frequency semicircle can be parameterized (for  $\omega < 0.01 \cdot D/(2 \cdot l^2)$ ) through:

$$Z(\omega) = Z_0 \frac{\frac{\tilde{D}}{l} + k}{\frac{\tilde{D}}{l} k + j \tilde{D} \omega} = Z_0 \frac{\left[ \frac{1}{k} + \frac{l}{\tilde{D}} \right] (1 - j \omega \frac{l}{k})}{1 + \omega^2 \left( \frac{l}{k} \right)^2} \quad (13)$$

which is the model of a capacitance parallel to a resistance:

$$R_{dc} = Z_0 \left[ \frac{1}{k} + \frac{l}{\tilde{D}} \right] \text{ and } C_{chem} = \frac{1}{Z_0 \left[ \frac{1}{l} + \frac{k}{\tilde{D}} \right]} \quad (14)$$

In case  $k \ll D$ , i.e. surface exchange limitation, then  $C_{chem}$  will be directly proportional to the thickness,  $l$ . The time constant,

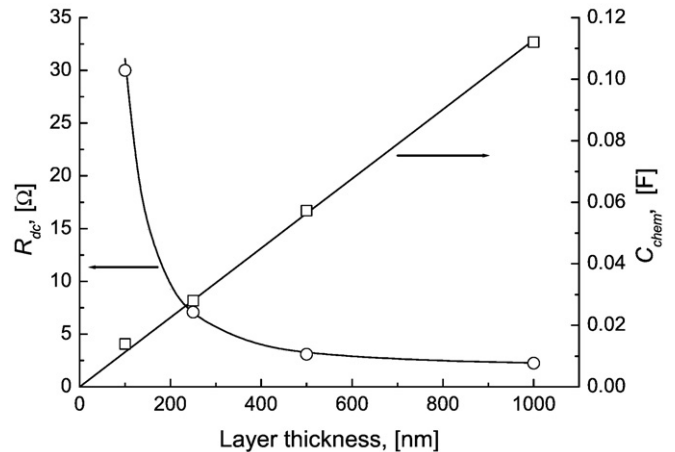


Fig. 6. Thickness dependence of  $R_{dc}$  and  $C_{chem}$ ,  $T=750$  °C in air.

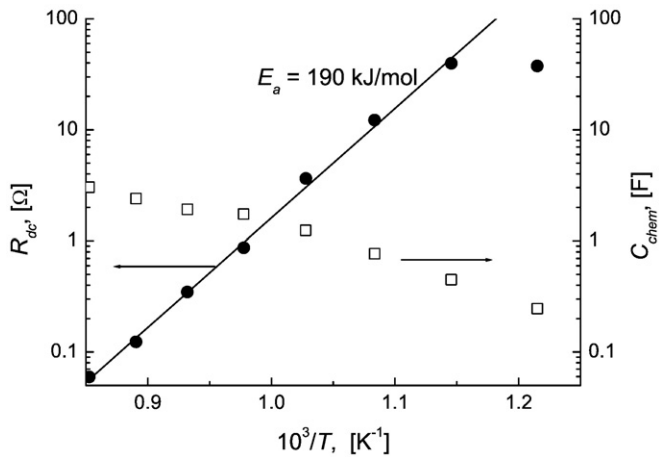


Fig. 7. Arrhenius graph of the surface exchange rate (presented as  $R_{pol}$ ) and  $C_{chem}$  for a 15  $\mu\text{m}$  thick PLD sample measured in air.

$\tau = R_{dc} \cdot C_{chem} = l/k$ , is independent of the diffusion coefficient.  $D$  can be obtained from the slope of  $R_{dc}$  vs.  $l$ .

### 3. Experimental procedure

Dense LSCF cathodes with different thickness were deposited by Pulsed Laser Deposition (PLD) on 2.5 mm thick  $\text{Ce}_{0.9}\text{Gd}_{0.1}\text{O}_{1.95}$  pellets in a three electrode arrangement, see Fig. 2. The pulsed laser deposition was performed with a KrF excimer laser, using a fluency of  $2.6 \text{ J/cm}^2$  and a frequency of 20 Hz. The LSCF target was an isostatically pressed LSCF pellet on a rotating holder. The laser ablation occurred in a vacuum chamber in 0.02 mbar oxygen ambient. The CGO substrates were heated to  $750^\circ\text{C}$  during deposition. The reference electrode was provided by a Pt wire bonded with a little Pt-ink into a groove at half height at the cylindrical side of the pellet. For the counter electrode a similar PLD layer with different thickness was applied. The use of a porous Pt-counter electrode is not advisable as the electrode properties are inferior to the LSCF electrodes and will result in a strong pseudo-inductive artifact in the impedance, see Fig. 3. This is the result of a cross-talk between counter and reference electrode (see e.g. [10]), caused by the excessive polarization of the Pt-counter electrode.

The electrode impedance was measured with a Solartron 1250 FRA combined with a 1287 electrochemical interface over a frequency

range of 65535 Hz to 10 mHz. The data is validated with a Kramers-Kronig test [11] and analysed with CNLS-program 'Equivalent Circuit'[12]. Thickness dependent measurements were carried out at  $750^\circ\text{C}$  in air. The impedance was also measured as function of temperature for a 15  $\mu\text{m}$  thick layer.

### 4. Results and discussion

Fig. 4 shows a close up of the PLD electrode and a SEM micrograph of the surface area. The typical impedance of a 1  $\mu\text{m}$  thick electrode is presented in Fig. 5. The high frequency Warburg behavior cannot be observed. The analysis results for  $R_{dc}$  and  $C_{chem}$  are presented in Fig. 6. The chemical capacitance shows a clear linear thickness dependence, which is consistent with surface exchange limitation, i.e.  $k \ll D$ , see Eq. (14). The electrode resistance  $R_{dc}$ , however, seems to be inversely proportional to the electrode thickness, which is neither consistent with diffusion limitation nor with surface exchange limitation. The observed dependence can be modeled (see Fig. 6) with:

$$R_{dc} = R_{exch} + R_{electr} \cdot l^{-2} \quad (15)$$

with:  $R_{exch} = 2.0 \Omega$  ( $1.6 \Omega \cdot \text{cm}^2$ ) and  $R_{electr} = 2.9 \cdot 10^5 \Omega \cdot \text{nm}^{-2}$ . This effect is caused by the distance between contact points of the Pt-mesh with respect to the layer thickness. Because of the sheet resistance a significant polarization drop evolves along the surface from each contact point, causing a concentration/activity gradient. Hence the 'apparent effective' surface area for the exchange decreases with diminishing layer thickness. For the 100 nm layer the electrode impedance shows a more clearly diffusive behavior (depressed semicircle, close to  $45^\circ$ ) which is consistent with this proposed model. This effect will be further analyzed using a Finite Element Modeling approach. From these results it is at least evident that the surface exchange reaction is rate determining for the dense electrodes.

The temperature dependence for a 15  $\mu\text{m}$  thick sample is presented in Fig. 7. The activation energy for the surface exchange reaction is with  $190 \text{ kJ} \cdot \text{mol}^{-1}$  quite high, but consistent with previous and recent conductivity relaxation measurements [13,14].

A preliminary poisoning study was carried out by adding a small amount of chromium by PLD to a fresh LSCF surface. The surface analysis was performed with Low Energy Ion Scattering Spectroscopy (LEISS) at Calipso b.v., Eindhoven (now in Münster). This sample showed a large Sr peak and a small Cr peak. A 'pristine' sample, used as blanco, showed a more significant Cr peak, while the Sr peak virtually had disappeared, see Fig. 8. This PLD LSCF layer had been the first layer

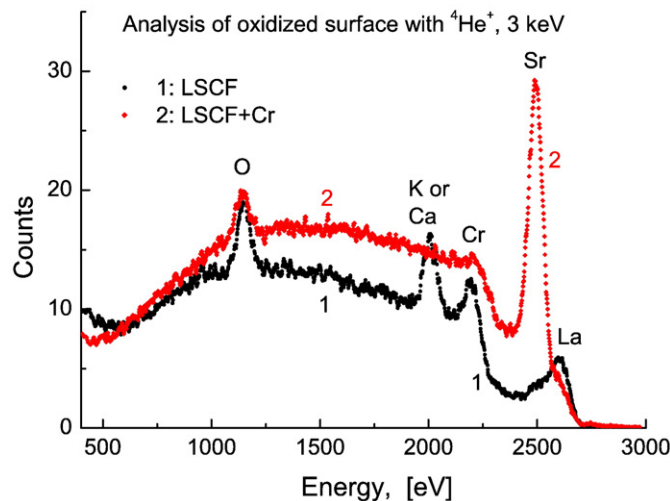


Fig. 8. LEIS spectrum of intentionally 'Cr-poisoned' LSCF surface (upper line) and pristine surface, but inadvertently poisoned by stainless steel heater plate (lower line).

deposited on the CGO electrolyte and, subsequently, had been in contact with the stainless steel heating plate on which the sample was mounted. This clearly indicates that chromium is easily transferred by contact. Two of the four layers had thus already a Cr surface contamination. The trend in the thickness dependence of  $R_{dc}$  does not indicate a serious influence of this Cr-poisoning, possibly indicating that more than a surface layer is needed for an appreciable effect.

## 5. Conclusions

The surface exchange rate of mixed conducting oxides can be studied easily on well-defined thin and dense layers deposited with pulsed laser deposition. Same type working and counter electrodes are strongly advised for a standard 3-electrode set-up. The polarization resistance of the counter electrode may not be significantly larger than the working electrode.

An important criterion for the minimal required thickness is the relation between the density of contact points (gauze mesh), the layer thickness, the electronic conductivity and the exchange rate. For the studied LSCF compound a minimum thickness of 1  $\mu\text{m}$  is required with the use of a standard Pt-gauze.

Great care must be taken during the PLD-procedure to avoid inadvertent contamination from the sample support/heater system. In direct contact chromium is already transferred from stainless steel to the backside of the cell.

## Acknowledgement

This research project was made possible through financial support from the Dutch Ministry of Economic Affairs through the EOS-SOFC programme.

## References

- [1] R.J. Chater, S. Carter, J.A. Kilner, B.C.H. Steele, *Solid State Ion.* 53–56 (1992) 859.
- [2] B.A. Boukamp, I.C. Vinke, K.J. de Vries, A.J. Burggraaf, in: B. Scrosati, A. Magistris, C.M. Mari, G. Mariotto (Eds.), *Fast Ion Transport in Solids*, NATO ASI Series, Series E: Appl. Sci., Vol. 250, Kluwer Academic, Dordrecht, 1993, p. 167.
- [3] H.J.M. Bouwmeester, C. Song, J. Zhu, J. Yi, M. van Sint Annaland, B.A. Boukamp, *Chem. Phys. Phys. Chem.* 11 (2009) 9640.
- [4] I. Yasuda, M. Ishinuma, in: T.A. Ramanarayanan, W.L. Worrell, H.L. Tuller (eds) *Proceedings of the 2nd Int. Symp. on ionic and mixed conducting ceramics* (Electrochem. Soc. proceedings series PV 1994-12, Pennington NJ, 1994) pp 209.
- [5] J.E. ten Elshof, M.H.R. Lankhorst, H.J.M. Bouwmeester, *Solid State Ion.* 99 (1997) 15.
- [6] B.A. Boukamp, M.W. den Otter, H.J.M. Bouwmeester, *J. Solid State. Electrochem.* 8 (2004) 592.
- [7] G.T. Kim, S. Wang, A.J. Jacobson, Z. Yuan, C. Chen, *J. Mater. Chem.* 17 (2007) 1316.
- [8] M.D. Levi, Z. Lu, D. Aurbach, *Solid State Ion.* 143 (2001) 309.
- [9] M. Mohamedi, D. Takahashi, T. Uchiyama, T. Itoh, M. Nishizawa, I. Uchida, *J. Power Sources* 93 (2001) 93.
- [10] B.A. Boukamp, *Solid State Ion.* 143 (2001) 47.
- [11] B.A. Boukamp, *J. Electrochem. Soc.* 142 (6) (1995) 1885.
- [12] B.A. Boukamp, *Solid State Ion.* 20 (1986) 31.
- [13] H.J.M. Bouwmeester, W.M. den Otter, B.A. Boukamp, *J. Solid State Electrochem.* 8 (2004) 599.
- [14] E. Bucher, W. Sitte, *Solid State Ion.* (2010), doi:10.1016/j.ssi.2010.01.006.